Comment on “Microhydration of Biomolecules: Revealing the Native Structures by Cold Ion IR Spectroscopy”

Summer L. Sherman, Kathleen A. Nickson, and Etienne Garand*

Department of Chemistry, University of Wisconsin-Madison, 1101 University Avenue, Madison, WI 53706, United States

*Author to whom correspondence should be addressed.

email: egarand@wisc.edu

Abstract

This paper presents a re-examination of the conclusions of a study reported in *The Journal of Physical Chemistry Letters* (Saparbaev et al., 2021, 12, 907) that compared the structure of microsolvated ions formed by electrospray ionization to those formed in the gas-phase via a previously published cryogenic ion trap approach. We conducted additional experiments that clearly show that most of the observed differences in the IR spectra can be accounted for by considering the different spectroscopic action schemes used to obtain them. In particular, the presence of the D_2-tag induces shifts in some of the N-H and O-H peaks which need to be carefully considered before comparing spectra. Once these spectral effects are taken into account, we show that both clustering approaches yields similar clusters structures for the small $GlyH^+(H_2O)_n$ species. Using unimolecular reaction rate theory, we also show that for the small complexes considered here, only the gas-phase equilibrium distribution of conformers should be expected in both experimental approaches. In addition, the barrier heights necessary to kinetically trap high-energy conformers at 298K is explored using a series of model polyalanine chains.

The manuscript by Saparbaev et al.[1] aimed to compare the structure of microhydrated protonated glycine [$GlyH^+(H_2O)_n$] and triglycine [$Gly_3H^+(H_2O)$] clusters produced by two different approaches. In their experiment, clusters were formed directly by soft electrospray ionization ("soft-ESI" thereafter) and thermalized in a room temperature storage ion trap for 45 ms before they were cooled to 6K in a cryogenic ion trap prior to spectroscopic interrogation. The infrared spectra of these clusters were directly compared to those previously obtained by our group,[2-5] in which the same species were formed by clustering H_2O onto the bare $GlyH^+$ or Gly_3H^+ ions in an 80K ion trap ("clustering approach" thereafter).[6] The clusters were then cooled to 10K in a cryogenic ion trap and D_2-tagged prior to spectroscopic interrogation. The observed differences in the $GlyH^+(H_2O)_{1-3}$ spectra of the species produced by either method led Saparbaev et al. to conclude that some of the conformers identified in the clustering approach were kinetically trapped "intrinsic gas-phase conformers", while all of those observed directly from soft-ESI must be the "native solution structures". Such kinetic trapping of solution-phase structures, or high-energy gas-phase structures, via soft-ESI has been observed numerous times previously.[7-13]

Here, we show that most of the observed differences in the IR spectra can be accounted for by considering the different spectroscopic action schemes used to obtain them. The species formed by the clustering approach were probed using infrared predissociation (IRPD) of the D_2-tagged species[14-15] while the soft-ESI clusters were probed by infrared multiple photon dissociation (IRMPD). Both schemes are indirect action spectroscopies that require careful considerations when analyzing the resulting spectra. For the one-photon IRPD experiment, while the effects of the D_2 presence are usually quite small, its interaction with specific N-H and O-H groups can nonetheless cause a ~10-50 cm^{-1} redshift in their infrared vibrational bands.[14, 16-17] The H_2O binding energy in $GlyH^+(H_2O)$ is calculated (cam-B3LYP/def2TZVP) to be around 6500 cm^{-1}

(77.8 kJ/mol), and therefore the IRMPD scheme requires the absorption of 2-3 photons in the 2900-3800 cm^{-1} range studied by Saparbaev et al. The potential changes in absorption cross-section after the absorption of the first photons, or variation in the rate of vibrational energy redistribution, may cause the intensity of features in IRPD and IRMPD spectra to differ.[18-19] The multiphoton nature of the IRMPD process can also make it more sensitive towards the higher energy kinetically-trapped conformers that require less photons for dissociation.

We have reacquired the IR spectra of the $GlyH^+(H_2O)_{1-3}$ clusters, using the exact same 80K ion trap clustering approach used in Ref 2-3, but this time we probed them using the same IRMPD scheme as Saparbaev et al. The resulting IR spectra are shown in the top panel of **Figure 1-3** (black trace) and compared to those of Saparbaev et al. (red trace). The D_2-tagged IRPD spectra from Ref 2-3 (blue trace) are also included for comparison. All spectra in the figures have been normalized to the common H_2O sym. stretch around 3630-3650 cm^{-1} peak to show differences in intensities. Some of the differences between the spectra of the ion trap clustering species acquired with IRPD and IRMPD highlights the perturbations induced by the D_2-tag. We recognize that our previous work did not adequately describe the inferred effects of the D_2 tag on the spectra and that this might have affected the interpretation of Saparbaev et al. Here, we will use the D_2-tagged IRPD and IRMPD spectra acquired under the same conditions to highlights these perturbations.

In **Figure 1**, the peak at 3340 cm^{-1} in the $GlyH^+(H_2O)$ IRPD spectrum which is absent in the IRMPD spectrum, can be attributed to a redshift of one of the N-H stretches resulting from direct interactions with the D_2 tag. In our previous work, we assigned the observed spectrum to the presence of two conformers, I-A and I-B, whose structures, and calculated spectra (without D_2 tag) are shown in **Figure 1**. These two conformers are necessary to explain the presence of small peaks at 3080 cm^{-1} and 3277 cm^{-1}. Because conformer I-A only has one free N-H, the addition of a D_2-tag is expected to redshift it and therefore the peak at 3339 cm^{-1} was explicitly assigned to I-A. Conformer I-B has two free N-H, and therefore should exhibit at least one mostly unperturbed N-H which led us to assign the highest N-H feature at 3357cm^{-1} to this conformer. In the absence of D_2-tag, the calculation predicts that these two features should be overlapping, consistent with the single peak at 3360 cm^{-1} in both IRMPD shown in **Figure 1**. We note that the IRMPD of Saparbaev et al. also exhibits peaks at 3080 cm^{-1} and 3277 cm^{-1}, consistent with the presence of the same I-A and I-B conformers in their experiment.

The assignment is not as straightforward for the $GlyH^+(H_2O)_2$ spectrum. In our previous work, we identified the presence of 3 conformers, II-A, II-B and II-D, which are shown in **Figure 2**. The presence of ~15% of II-D, in which the water interacts with the carboxylic acid O-H, was confirmed and quantified with the observation of its unique C=O stretch at 1757 cm^{-1} (not shown here, see Ref 3). The remaining ~85% conformer population was assigned to conformers II-A and II-B. In Ref 3, isomer-specific IR-IR double resonance was used to confirmed that the two peaks at 3313 cm^{-1} and 3344 cm^{-1} belong to separate conformers. Because both II-A and II-B only have one free N-H, we would expect them to be redshifted by the presence of a D_2-tag. Unfortunately, the signal/noise ratio in our IRMPD spectra is not sufficient to clearly identify the position of these N-H stretches without the D_2-tag. However, the IRMPD of Saparbaev et al. clearly show a feature at 3375 cm^{-1} which is consistent with the calculated spectra of II-A, II-B, and II-D. Here the presence of multiple conformers with similar IR spectra makes it difficult to conclusively compare the conformers produced by both clustering methods.

Finally, in the $GlyH^+(H_2O)_3$ spectra shown in **Figure 3**, the presence of the D_2-tag redshift the carboxylic O-H feature from 3560 cm^{-1} in the IRMPD spectrum to 3538 cm^{-1} in the D_2-tagged spectrum. In our previous work, we identify the presence of 4 conformers for $GlyH^+(H_2O)_3$, which are shown in **Figure 3**. Conformer III-D, in which all three waters are bound to the NH_3^+ group, is the only one that can give rise to the observed carboxylic acid O-H near 3550 cm^{-1}. Because the N-H groups are completely occupied by the water molecules, the most likely D_2-tagging site is the carboxylic acid O-H, consistent with the shifted frequency of this feature in the D_2-tagged IRPD spectrum. In our previous work, the small peaks at 3312 cm^{-1} and 3349 cm^{-1} were assigned to the presence of conformers III-B and III-A, respectively. Finally, the presence of conformer III-C, which does not exhibit any unique features, could not be ruled out. Using the calculated relative intensities of all the conformers, we estimated that the contribution of III-C is less than 10%. The IRMPD spectra of Saparbaev et al. clearly exhibit features at ~3315cm^{-1}, ~3355cm^{-1} and ~3560cm^{-1} which are consistent with the presence of the same III-A, III-B and III-D major conformers.

Overall, careful analysis of the spectra shows that similar $GlyH^+(H_2O)_n$ clusters structures are generated by both clustering methods. This conclusion is also supported by the unimolecular dynamic analysis presented in the next section. Another important conclusion is that careful analysis is always required in order to directly compare action IR spectra produced by different schemes. The spectral features shouldn't be directly compared, but rather the resulting structures obtained from properly analyzing them within their respective framework. We also note that the IRMPD of the same species acquired in each lab (black and red traces) show some marked difference in peak intensities. For example, in $GlyH^+(H_2O)$ the carboxylic O-H peak at 3550 cm^{-1} is a lot more intense in the black trace. In $GlyH^+(H_2O)_2$ and $GlyH^+(H_2O)_3$, the N-H peak between 3300-3400 cm^{-1} is a lot weaker and sometime barely visible in the black traces. These could be due to saturation effects, different signal to noise ratios, and mostly different laser fluence between the two experiments. It highlights once again that direct comparison between action spectra must always be done carefully. While experimentally more demanding, the IR-IR two-color approach pioneered by Y.T. Lee and co-workers[20] and recently adapted by Yang et. al.[21] might provide vibrational spectra of mass-selected ions which are free tag perturbation and non-linear effects and closer to the true linear absorption spectra.

The results that both cluster formation schemes essentially yield similar conformers for the $GlyH^+(H_2O)_n$ clusters is not too surprising given the very small barriers between the structures labeled as "native solution structure" and "intrinsic gas-phase conformer" by Saparbaev et al. (see **Figure 4**), which were computed and presented in Ref 3. Conversion between these structures involve a simple C-N bond rotation with calculated barriers of ~1.2 kJ/mol for $GlyH^+(H_2O)_1$ and ~9.0 kJ/mol for $GlyH^+(H_2O)_2$. For reference, the average vibrational internal energies, calculated using harmonic frequencies, is 15.0 kJ/mol and 24.5 kJ/mol for $GlyH^+(H_2O)_1$ and $GlyH^+(H_2O)_2$ at 298K, respectively. Using Rice-Ramsperger-Kassel-Marcus (RRKM) theory[22] of unimolecular reaction rates, we can roughly estimate that the half-life for the conversion between the "native structure" and "intrinsic gas-phase conformer" would be less than 100 ps at 298K. These barriers are simply too small to prevent interconversion at room temperature for 45 ms, as in the experiment of Saparbaev et al.

For relatively small species such as $GlyH^+(H_2O)_2$, the fast unimolecular dynamics means that kinetic trapping of conformers is unlikely to occur on the millisecond experimental timescale unless the activation barrier is very close to, or larger than, the vibrational internal energy. This is illustrated in **Figure 5**, which shows the half-life of a $GlyH^+(H_2O)_2$ conformer at room temperature as a function of a hypothetical interconversion barrier height. For an internal energy of 24.5 kJ/mol, half-lives shorter than 1 μs are found for all barrier height smaller than ~23 kJ/mol. For increasingly more complex species or larger clusters, the rate of unimolecular reaction would decrease due to the large increase in vibrational state density. However, the vibrational internal energy available at room temperature will also increase with vibrational state density. To look at these competing effects, we computed the harmonic vibrational state density and unimolecular reaction rate of simple linear polyalanine peptide chains with 3-20 monomers. The distribution of vibrational states of the hypothetical conformer conversion transition-state was approximated to be the same as the reactant structure but shifted by the height of the arbitrary barrier. The average vibrational internal energy at 298K, shown in **Figure 6a**, scales almost linearly from 40 kJ/mol to 295 kJ/mol when the chain length is increased from 3 to 20 monomers. **Figure 6b** (black trace) shows the minimum conversion barrier height necessary to produce conformer half-life of at least 50 ms at 298K as a function of the number of monomers. For the smallest $(Ala)_3$ species, the minimum barrier essentially corresponds to the available internal energy. However, for the larger species, the necessary barrier does not scale linearly with internal energy, but instead plateaus slightly above 60 kJ/mol for chains longer than 10 monomers. This implies that for the larger species, the conversion rate remains slow enough to produce kinetic trapping even at internal energies well above the barrier. We note that Zwier and co-workers[23] reached similar conclusions by applying similar RRKM calculations to the conversion of the protonated pentapeptide YGPAA in a cryogenic ion trap. The 50 ms timescale is representative of many experiments in which ions are stored at room temperature between each laser spectroscopy or ion mobility spectrometry characterization steps. An alternative approach that favors kinetic trapping in soft-ESI would be to cryogenically cool the ions immediately after the ESI step. To explore this possibility, we calculated the necessary barriers for producing a conformer half-life of 0.5 ms at 298K, as shown in **Figure 6b** (red trace). Despite a 100x shorter timescale, the required barrier heights are only reduced by less than 20%. This shows that the combination of internal energies and unimolecular reaction rates are the dominant factors in producing kinetically trapped structures. While the

RRKM calculations presented here are only crude estimates, they nevertheless provide a rough guide of when kinetic trapping should or should not be expected in soft-ESI.

A similar kinetic analysis can be made for the ion trap clustering approach. At first glance, it would appear to favor the formation of kinetically trapped structures due to its lower ~80K working temperature. However, we must consider that during the clustering process, the binding energy between the clustering H_2O molecule and the ion will be available as internal energy of the newly formed cluster. For the $GlyH^+ + H_2O$ complex, this binding energy is calculated to be ~77.8 kJ/mol, which is 5 times larger than the internal energy of the 298K cluster. The formation of kinetically trapped structures would require cooling of this excess energy on unrealistically short picosecond timescale. Using the inelastic collision model of Drahos and Vekey,[24] we estimate that the timescale for cooling at 1×10^{-4} torr to be on the order of milliseconds, which leaves ample time for conformer conversion. We have demonstrated previously[4] that for $Gly_3H^+(H_2O)$, a ~68 kJ/mol barrier between conformers could be overcome by the ~70 kJ/mol water binding energy during the clustering process at 80K, yielding predominantly the same lowest energy gas-phase conformer as the soft-ESI approach used by Saparbaev et al. Under the specific clustering conditions used in Ref 4, only 10% of the conformer population remained kinetically trapped. Once again, for the larger species, the slower unimolecular dynamics would increase the probability of kinetic trapping. Although we have not explored this possibility in detail yet, the fraction of kinetically trapped conformers could potentially be controlled by manipulating the ion trap buffer gas pressure and thus the cooling rate of the binding energy.

In summary, the analysis presented here suggests that for relatively small species, both soft-ESI and ion trap clustering approach are likely to yield a conformer distribution determined by gas-phase equilibrium energetics, unless the interconversion barriers are larger than the H_2O

binding energy (clustering approach) or the internal energy at room temperature (soft-ESI). The slower unimolecular dynamics in the larger species and clusters would favor the formation of kinetically trapped species in both cases. Finally, we note that one largely unexplored aspect of cryogenic ion trap spectroscopy, common to both approaches discussed here, is the effect of buffer gas cooling on conformer distributions. The fact that multiple conformers are routinely observed after cooling to below 10K suggests that the collisional cooling is sufficiently fast for preserving some of the more entropically-favored conformations. However, it is unclear whether the final observed conformer distribution is representative of the room-temperature equilibrium or an intermediate temperature. Moreover, the extent of observed kinetic trapping is likely to be highly dependent on cooling rate and specific experimental conditions, which will all need to be characterized when comparing results from different laboratories.

Acknowledgments

This work was supported by the US Department of Energy, Office of Science, Basic Energy Sciences, under award no. DE-SC0018902. The computational resources used in this work are supported by National Science Foundation grant CHE-0840494. This material is based upon work supported by the National Science Foundation Graduate Research Fellowship under Grant No. DGE-1747503. Any opinions, findings, and conclusions or recommendations expressed in this material are those of the author(s) and do not necessarily reflect the views of the National Science Foundation. Support was also provided by the Graduate School and the Office of the Vice Chancellor for Research and Graduate Education at the University of Wisconsin-Madison with funding from the Wisconsin Alumni Research Foundation.

References

(1) Saparbaev, E.; Aladinskaia, V.; Zviagin, A.; Boyarkin, O. V. Microhydration of Biomolecules: Revealing the Native Structures by Cold Ion IR Spectroscopy. *J Phys Chem Lett* **2021,** *12* (2), 907-911.

(2) Fischer, K. C.; Sherman, S. L.; Garand, E. Competition between Solvation and Intramolecular Hydrogen-Bonding in Microsolvated Protonated Glycine and beta-Alanine. *J Phys Chem A* **2020,** *124* (8), 1593-1602.

(3) Fischer, K. C.; Sherman, S. L.; Voss, J. M.; Zhou, J.; Garand, E. Microsolvation Structures of Protonated Glycine and l-Alanine. *J Phys Chem A* **2019,** *123* (15), 3355-3366.

(4) Fischer, K. C.; Voss, J. M.; Zhou, J.; Garand, E. Probing Solvation-Induced Structural Changes in Conformationally Flexible Peptides: IR Spectroscopy of Gly3H(+).(H2O). *J Phys Chem A* **2018,** *122* (41), 8213-8221.

(5) Voss, J. M.; Fischer, K. C.; Garand, E. Revealing the structure of isolated peptides: IR-IR predissociation spectroscopy of protonated triglycine isomers. *Journal of Molecular Spectroscopy* **2018,** *347*, 28-34.

(6) Marsh, B. M.; Voss, J. M.; Garand, E. A dual cryogenic ion trap spectrometer for the formation and characterization of solvated ionic clusters. *J Chem Phys* **2015,** *143* (20), 204201.

(7) Cao, W.; Zhang, H.; Yuan, Q.; Zhou, X.; Kass, S. R.; Wang, X. B. Observation of Conformational Simplification upon N-Methylation on Amino Acid Iodide Clusters. *J Phys Chem Lett* **2021,** *12* (11), 2780-2787.

(8) Zhang, H.; Cao, W.; Yuan, Q.; Zhou, X.; Valiev, M.; Kass, S. R.; Wang, X. B. Cryogenic "Iodide-Tagging" Photoelectron Spectroscopy: A Sensitive Probe for Specific Binding Sites of Amino Acids. *J Phys Chem Lett* **2020,** *11* (11), 4346-4352.

(9) Fernandez-Lima, F. A.; Becker, C.; Gillig, K. J.; Russell, W. K.; Tichy, S. E.; Russell, D. H. Ion mobility-mass spectrometer interface for collisional activation of mobility separated ions. *Anal Chem* **2009,** *81* (2), 618-24.

(10) Hoaglund-Hyzer, C. S.; Lee, Y. J.; Counterman, A. E.; Clemmer, D. E. Coupling ion mobility separations, collisional activation techniques, and multiple stages of MS for analysis of complex peptide mixtures. *Anal Chem* **2002,** *74* (5), 992-1006.

(11) Masson, A.; Kamrath, M. Z.; Perez, M. A.; Glover, M. S.; Rothlisberger, U.; Clemmer, D. E.; Rizzo, T. R. Infrared Spectroscopy of Mobility-Selected H+-Gly-Pro-Gly-Gly (GPGG). *J Am Soc Mass Spectrom* **2015,** *26* (9), 1444-54.

(12) Voronina, L.; Masson, A.; Kamrath, M.; Schubert, F.; Clemmer, D.; Baldauf, C.; Rizzo, T. Conformations of Prolyl-Peptide Bonds in the Bradykinin 1-5 Fragment in Solution and in the Gas Phase. *J Am Chem Soc* **2016,** *138* (29), 9224-33.

(13) Voronina, L.; Rizzo, T. R. Spectroscopic studies of kinetically trapped conformations in the gas phase: the case of triply protonated bradykinin. *Phys Chem Chem Phys* **2015,** *17* (39), 25828-36.

(14) Kamrath, M. Z.; Garand, E.; Jordan, P. A.; Leavitt, C. M.; Wolk, A. B.; Van Stipdonk, M. J.; Miller, S. J.; Johnson, M. A. Vibrational characterization of simple peptides using cryogenic infrared photodissociation of H2-tagged, mass-selected ions. *J Am Chem Soc* **2011,** *133* (16), 6440-8.

(15) Wolk, A. B.; Leavitt, C. M.; Garand, E.; Johnson, M. A. Cryogenic ion chemistry and spectroscopy. *Acc Chem Res* **2014,** *47* (1), 202-10.

(16) Tsybizova, A.; Paenurk, E.; Gorbachev, V.; Chen, P. Perturbation of Pyridinium CIVP Spectra by N2 and H2 Tags: An Experimental and BOMD Study. *J Phys Chem A* **2020,** *124* (41), 8519-8528.

(17) Masson, A.; Williams, E. R.; Rizzo, T. R. Molecular hydrogen messengers can lead to structural infidelity: A cautionary tale of protonated glycine. *J Chem Phys* **2015,** *143* (10), 104313.

(18) Eyler, J. R. Infrared multiple photon dissociation spectroscopy of ions in Penning traps. *Mass Spectrom Rev* **2009,** *28* (3), 448-67.

(19) Oomens, J.; Sartakov, B. G.; Meijer, G.; von Helden, G. Gas-phase infrared multiple photon dissociation spectroscopy of mass-selected molecular ions. *International Journal of Mass Spectrometry* **2006,** *254* (1-2), 1-19.

(20) Yeh, L. I.; Okumura, M.; Myers, J. D.; Price, J. M.; Lee, Y. T. Vibrational spectroscopy of the hydrated hydronium cluster ions H3O+·(H2O)n (n=1, 2, 3). *The Journal of Chemical Physics* **1989,** *91* (12), 7319-7330.

(21) Yang, N.; Duong, C. H.; Kelleher, P. J.; Johnson, M. A.; McCoy, A. B. Isolation of site-specific anharmonicities of individual water molecules in the I−·(H2O)2 complex using tag-free, isotopomer selective IR-IR double resonance. *Chemical Physics Letters* **2017,** *690*, 159-171.

(22) Callear, A. B. Chapter 4 Basic RRKM Theory**1983,** *24*, 333-356.

(23) Harrilal, C. P.; DeBlase, A. F.; Fischer, J. L.; Lawler, J. T.; McLuckey, S. A.; Zwier, T. S. Infrared Population Transfer Spectroscopy of Cryo-Cooled Ions: Quantitative Tests of the Effects of Collisional Cooling on the Room Temperature Conformer Populations. *J Phys Chem A* **2018,** *122* (8), 2096-2107.

(24) Drahos, L.; Vekey, K. MassKinetics: a theoretical model of mass spectra incorporating physical processes, reaction kinetics and mathematical descriptions. *J Mass Spectrom* **2001,** *36* (3), 237-63.

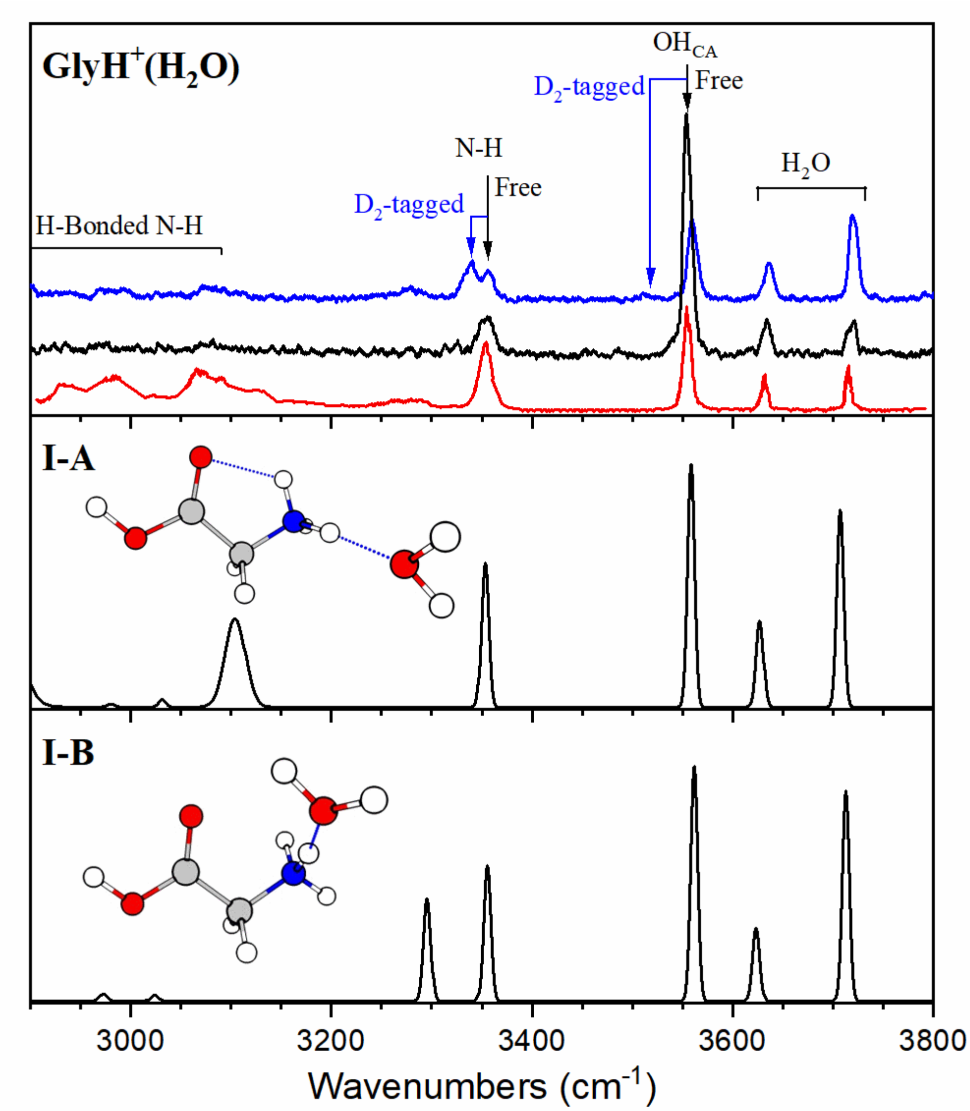

Figure 1. (Top Panel) IRMPD spectra of $GlyH^+(H_2O)$, produced through clustering approach (black trace; this work) and soft-ESI (red trace; Saparbaev et al.[1]). IRPD spectra of $GlyH^+{\cdot}D_2(H_2O)$, produced via clustering approach (blue trace; previous work[2-3]). All traces are normalized to their respective free O-H water sym. stretch between 3630-3650 cm^{-1}. (Bottom Panels) Harmonic spectra calculated at the cam-B3LYP/def2TZVP/GD3BJ level.

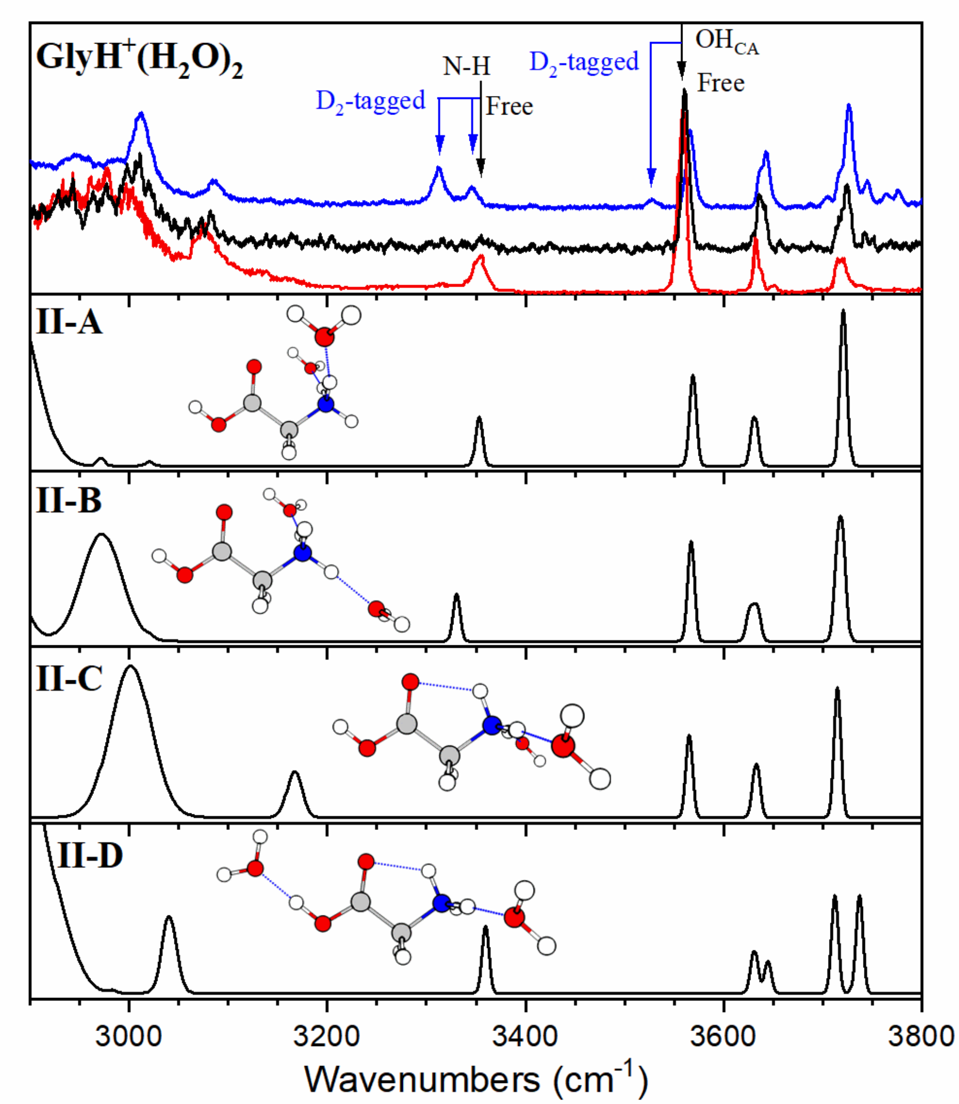

Figure 2. (Top Panel) IRMPD spectra of $GlyH^+(H_2O)_2$, produced through clustering approach (black trace; this work) and soft-ESI (red trace; Saparbaev et al.[1]). IRPD spectra of $GlyH^+\cdot D_2(H_2O)_2$, produced via clustering approach (blue trace; previous work[2-3]). All traces are normalized to their respective free O-H water sym. stretch between 3630-3650 cm^{-1}. (Bottom Panels) Harmonic spectra calculated at the cam-B3LYP/def2TZVP/GD3BJ level.

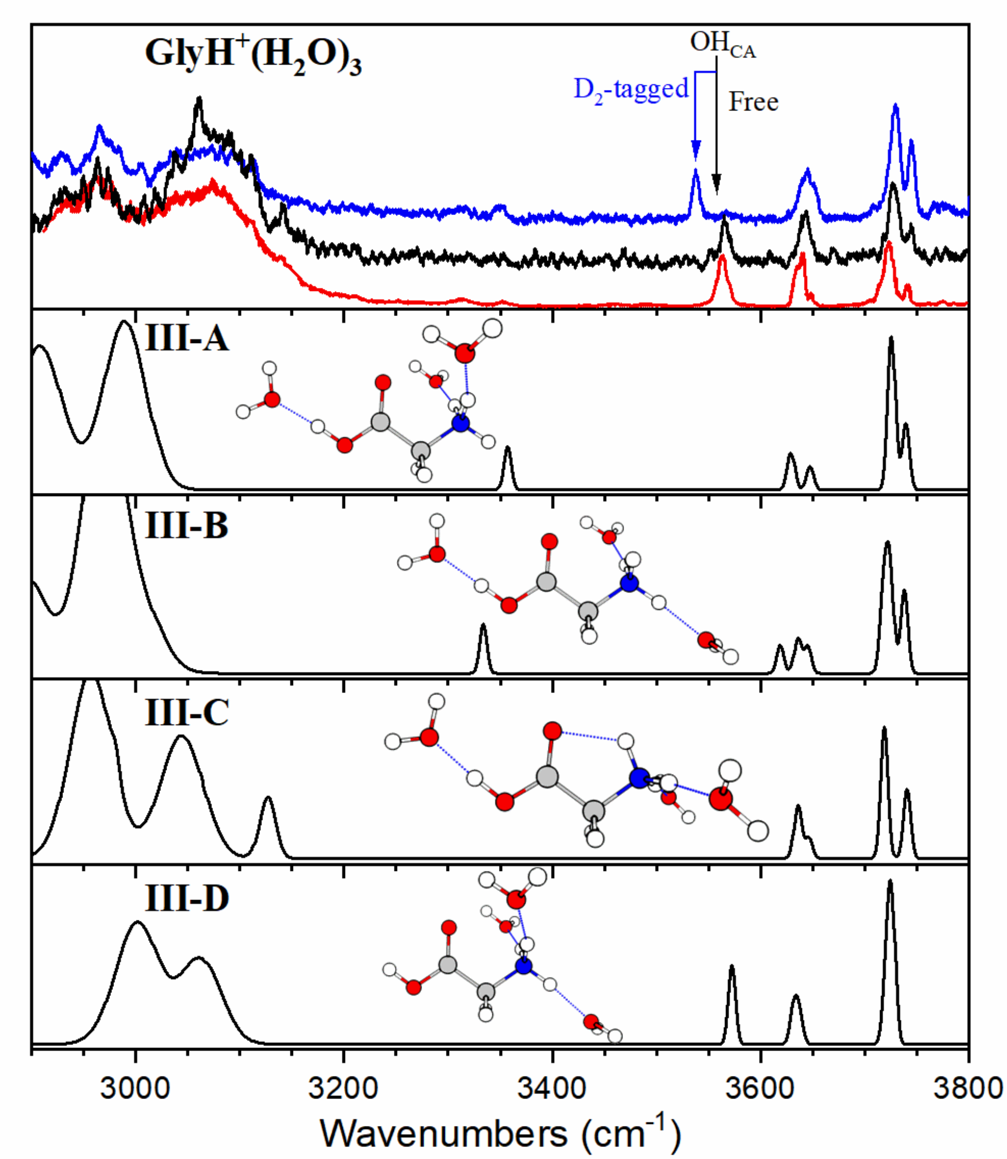

Figure 3. (Top Panel) IRMPD spectra of $GlyH^+(H_2O)_3$, produced through clustering approach (black trace; this work) and soft-ESI (red trace; Saparbaev et al.[1]). IRPD spectra of $GlyH^+ \cdot D_2(H_2O)_3$, produced via clustering approach (blue trace; previous work[2-3]). All traces are normalized to their respective free O-H water sym. stretch between 3630-3650 cm^{-1}. (Bottom Panels) Harmonic spectra calculated at the cam-B3LYP/def2TZVP/GD3BJ level.

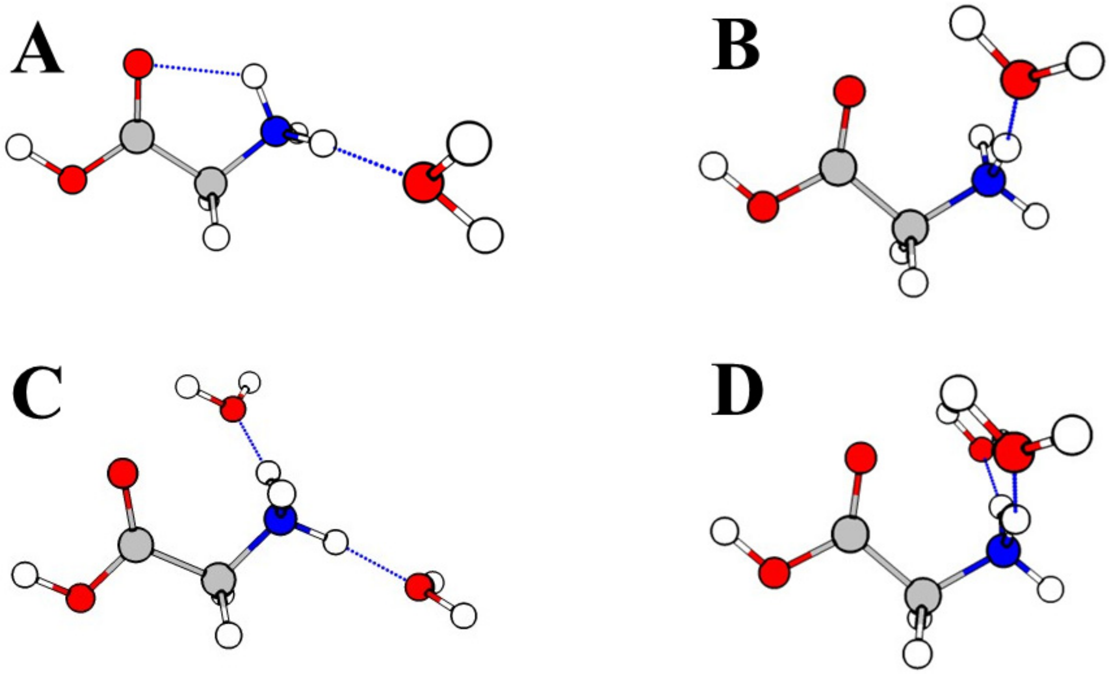

Figure 4. $GlyH^+(H_2O)$ labeled as (A) “intrinsic gas-phase” and (B) “native solution-phase” form as labeled by Saparbaev et al.[1] $GlyH^+(H_2O)_2$ in its (C) “intrinsic gas-phase” and (D) “native” form.

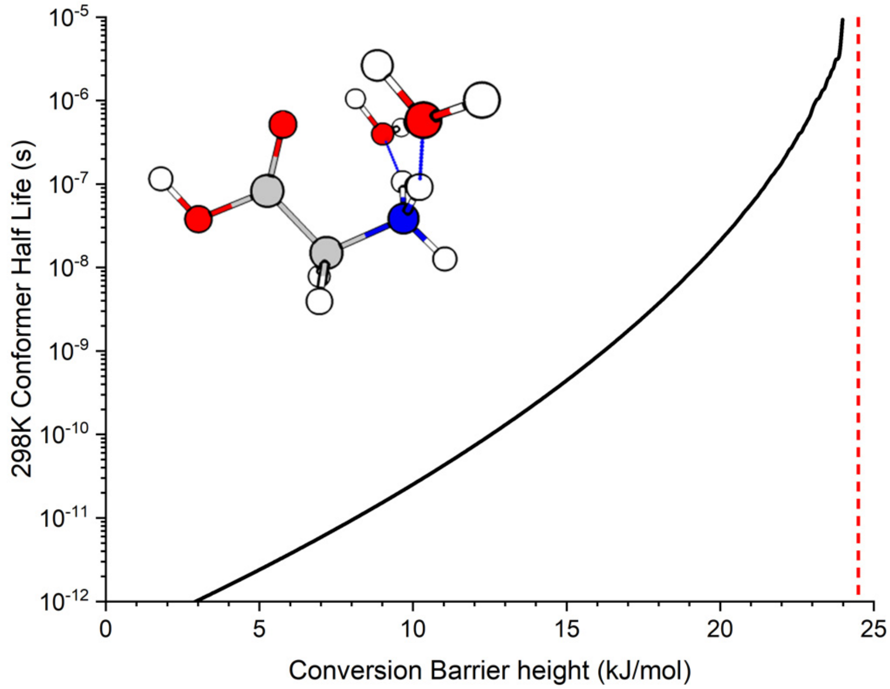

Figure 5. The calculated half-life of a $GlyH^{+}(H_2O)_2$ conformer at room temperature as a function of the conversion barrier height. The red dotted line marks the internal energy of $GlyH^{+}(H_2O)_2$ at 298K.

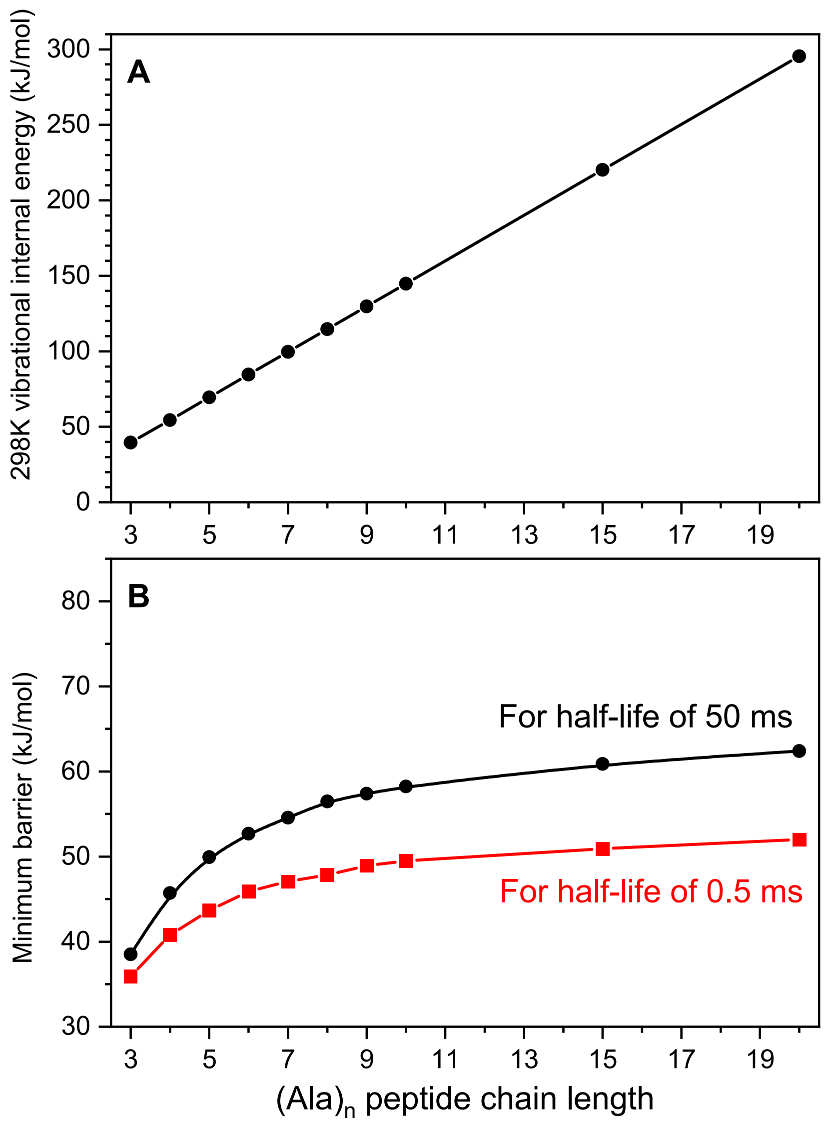

Figure 6. (A) The calculated average vibrational internal energy at 298K for linear polyalanine peptide chains with 3-20 monomers. (B) The minimum conversion barrier height necessary to produce a conformer half-life of at least 50ms (black trace) or 0.5ms (red trace) at 298K as a function of the number of monomers.

Table of content figure